PLASTIC HINGE MODEL OF REINFORCED CONCRETE COUPLING BEAMS

Hyeon-Jong Hwang[1], Soo-Hyun KIM[2], Sung-Hyun KIM[3], Mok-In PARK[4], and Hong-Gun PARK[5]

SUMMARY

As inelastic deformation increases, shear strength of reinforced concrete coupling beams is degraded by diagonal cracking. For performance-based design of short coupling beams, this study proposed a shear strength degradation model based on diagonal strut and truss mechanisms. The effects of the target chord rotation, longitudinal rebar ratio, length-to-height ratio, ratio and details of transverse reinforcement, distributed longitudinal web bars, and diagonal bars were considered. Based on the proposed method, a simplified moment-rotation relationship of plastic hinges was developed for the nonlinear numerical analysis of coupling beams. The prediction of the proposed method was compared with existing coupling beam specimens. The predicted moment-rotation relationships generally agreed with the test results.

Keywords*: Coupling beam; Deformation capacity; Diagonal bars; Distributed bars; Performance based design; Shear strength.*

INTRODUCTION

In reinforced concrete (RC) coupled walls, coupling beams are the critical members that are subjected to high shear and inelastic deformation. As the l_w/l ratio increases, the chord rotation (θ) demand of the coupling beams is amplified to 2-4 times the lateral drift ratio (θ_w) of RC walls (**Fig. 1**). Thus, the rotation demand can reach a 2~6% drift ratio, according to the target performance and geometric properties. In the coupling beams with the shear span-to-depth ratio ≤ 2.0, the shear strength and deformation capacity can be limited by early shear failure. To evaluate the seismic performance of coupling beams with various conforming or nonconforming reinforcement details, the overall load-displacement relationship, including deformation capacity, needs to be accurately defined according to various details.

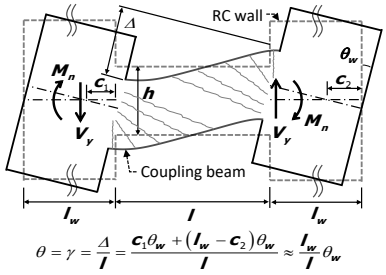

Fig. 1 Coupling beam in RC wall

For the performance-based design and evaluation of RC walls, FEMA 356 (2000) and ASCE/SEI 41-17 (2017) define the plastic deformation of coupling beam addressing the failure mode, rebar detail, and shear strength-to-demand ratio. Kanakubo et al. (1996) proposed a shear capacity index to estimate the deformation capacity of

[1] *Presenter, Associate Professor, School of Architecture, Konkuk University, Korea, email: hwanggun85@naver.com*
[2] *Graduate student, School of Architecture, Konkuk University, Korea, e-mail: kb9711@konkuk.ac.kr*
[3] *Post doctor, School of Architecture, Soongsil University, Korea, e-mail: jangson@snu.ac.kr*
[4] *Graduate student, Dept. of Architecture & Architectural Engineering, Seoul National University, Korea, e-mail: mokmok-p@snu.ac.kr*
[5] *Professor, Dept. of Architecture & Architectural Engineering, Seoul National University, Korea, e-mail: parkhg@snu.ac.kr*

coupling beams with l/h= 2.4 and 2.8. Hong and Jang (2006) estimated the deformation capacity of coupling beams by using a strain-based bond model and strut-tie mechanism. Eom et al. (2009) proposed an energy-based cyclic model for coupling beams, on the basis of a nonlinear truss model. Lee and Watanabe (2003), and Eom and Park (2013) evaluated the effect of longitudinal axial strain in the plastic hinge on the cyclic behavior of coupling beams. Naish et al. (2013) proposed the effective stiffness, deformation capacity, and residual strength of coupling beams, using a plastic hinge model. Lim et al. (2016) proposed a strut-tie model to predict the shear strength of coupling beams with l/h= 1.0-4.0. Godínez et al. (2021) considered the shear deformation and bar-slip to propose a stiffness modifier for the effective stiffness of coupling beams with diagonal reinforcement. Eom et al. (2022) estimated the effective stiffness combining flexural and shear deformations of coupling beams, and defined the deformation capacity as a function of the stirrup ratio. However, the strength degradation behavior of coupling beams was not clearly defined. Thus, to extend the applicability, a unified model is required to address the effects of various load transfer mechanisms and reinforcement details.

In the present study, the shear strength degradation of short coupling beams ($l/h \leq 2.5$) with conventional and/or diagonal reinforcement was evaluated. Based on the shear strength degradation model, a moment-rotation relationship for the nonlinear numerical analysis of short coupling beams was developed. For verification, the proposed method was compared with the existing test results.

PLASTIC HINGE MODEL FOR COUPLING BEAMS

Fig. 2(a) shows the proposed plastic hinge model for short coupling beams. A coupling beam consists of an elastic beam element, two rotational spring elements, and two rigid links. The rotational spring elements at the ends of the coupling beam describe the plastic deformation of the coupling beam. The rigid link is used to represent the rigid panel zone at the beam-wall joint. The elastic beam element describes the elastic flexural deformation and shear deformation of the coupling beam. Eom et al. (2022) proposed an effective flexural stiffness (E_cI_b) of coupling beams, considering the effects of the elastic flexural deformation and shear deformation.

$$E_cI_b = \frac{0.3}{1+20\left(h/l\right)^3} E_cI_g \tag{1}$$

where E_c = elastic modulus of concrete (= $4700\sqrt{f_c'}$ in MPa); I_g = second-order moment of inertia of the gross cross section in the coupling beam; h = coupling beam height; and l = coupling beam length.

Fig. 2(b) shows the moment-rotation relationship of a rotational spring element. In FEMA 356 (2000) and ASCE/SEI 41-17 (2017), depending on the failure mode (flexural failure and shear failure), rebar detail (longitudinal bar layout and stirrup spacing), and load condition (shear demand-to-strength ratio), the plastic rotation angles are defined as: a = inelastic deformation prior to a sudden strength degradation; b = ultimate deformation at failure; and c = residual strength. In short coupling beams with length-to-height ratio (l/h) ≤ 2.5, most of the inelastic deformation is caused by diagonal cracking. Thus, the rotational spring element mainly describes the inelastic deformation due to diagonal cracking. In this study, considering flexural yielding at both beam ends, rotational spring elements were applied to the two ends of the coupling beam. The moment-rotation relationship of the rotational spring element is defined by the shear strength degraded after flexural yielding.

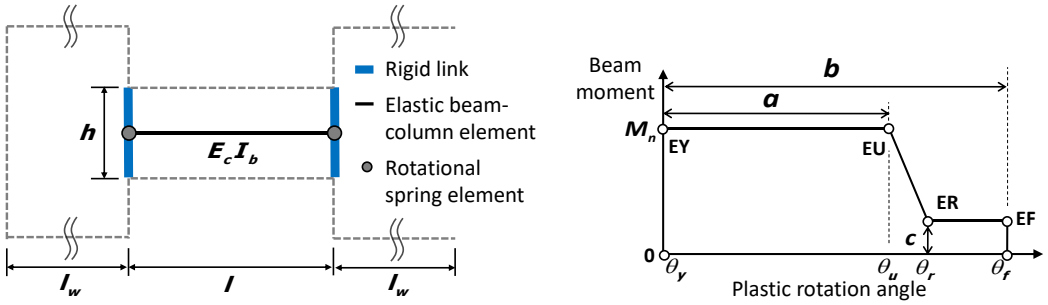

(a) Plastic hinge model for coupling beams (b) Envelope curve for rotational spring element

Fig. 2 Nonlinear analysis model for coupling beams

SHEAR STRENGTH DEGRADATION

Fig. 3 shows three shear resistance mechanisms of the short coupling beam with $l/h \leq 2.5$: 1) diagonal strut

mechanism resistance (V_C) developed by the bearing stress of the beam end; 2) truss mechanism resistance (V_T) developed by the bond force of longitudinal bars and the tensile force of transverse reinforcement; and 3) diagonal bar resistance (V_D).

$$V_n = V_C + V_T + V_D \tag{2}$$

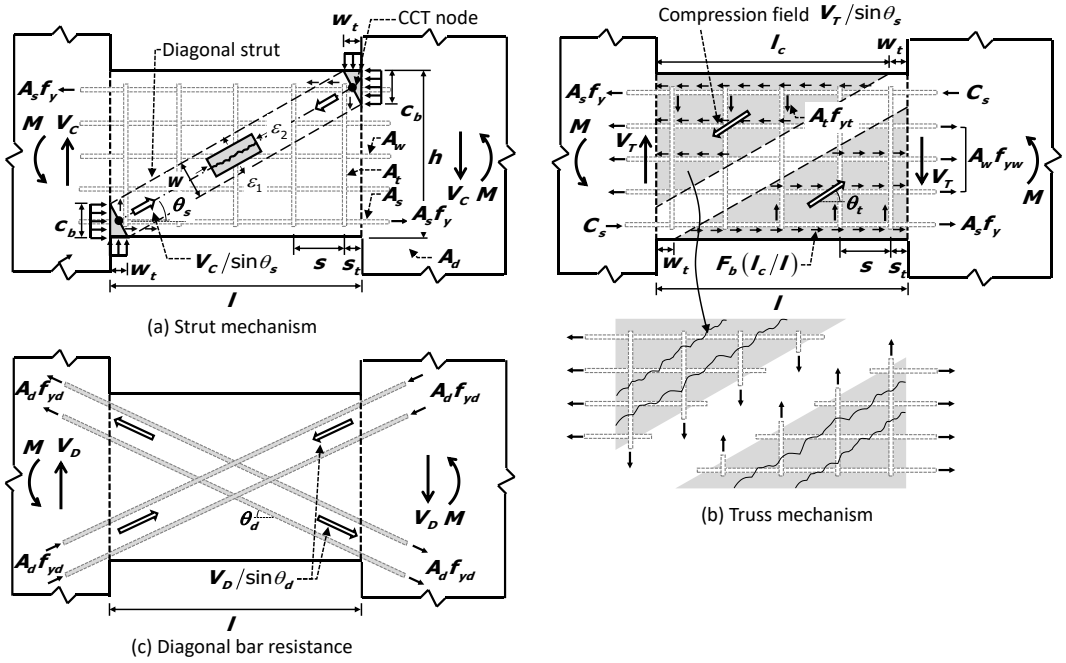

Fig. 3 Shear resistance mechanisms of short coupling beam

Diagonal strut resistance V_C

The shear resistance V_C of the diagonal strut is determined by the compressive strength of the diagonal strut that is formed by the flexural compression zone of the coupling beam. The compression zone depth c_b can be defined as follows:

$$c_b = \frac{A_s f_y + A_d f_{yd} \cos\theta_d}{0.85 f_c' b} \tag{3}$$

where A_s = area of the flexural tension rebars of the beam section; f_y = yield strength of the flexural tension rebars; f_c' = concrete strength; b = coupling beam width; A_d = area of the diagonal bars; f_{yd} = yield strength of the diagonal bars; and θ_d = inclined angle of the diagonal bars.

As shown in **Fig. 3(a)**, a CCT node is formed by the transverse reinforcement in the interface between beam and wall. According to ACI 318-19 (2019), the maximum width w_t of the CCT node is defined as follows:

$$w_t = \frac{A_t f_{yt}}{0.8(0.85 f_c')b} \le 2s_t \tag{4}$$

where A_t = area of the transverse reinforcement at a single layer; f_{yt} = yield strength of the transverse reinforcement; and s_t = distance between the wall face and the first transverse reinforcement layer, which should be not more than 50 mm.

In **Fig. 3(a)**, the width w of the diagonal strut is defined as follows:

$$w = c_b \cos\theta_s + w_t \sin\theta_s \tag{5}$$

The angle (θ_s) of the diagonal strut was determined from the geometric property and crack angle based on existing test results.

$$\theta_s = \text{atan}\left(\frac{h - c_b}{l - w_t}\right) \tag{6}$$

Following MCFT (1986) and assuming a uniform strain field in the web of coupling beams, the effective concrete compressive strength fce of the diagonal strut is determined from the principal tensile strain ε_1 in the web (Hwang et al. 2017, 2019, 2020, 2021).

$$f_{ce} = \frac{f_c'}{0.8+170\varepsilon_1} \approx \frac{f_c'}{0.8+170\left[\frac{\gamma}{2}\tan\theta_s + \varepsilon_{yt}\right]} \le f_c' \tag{7}$$

where γ = inelastic shear distortion of the coupling beam; and ε_{yt} = yield strain of the transverse reinforcement (i.e. the transverse reinforcement is assumed to yield at shear failure after beam yielding).
The shear resistance V_C of the diagonal strut is defined as the vertical component of the strut strength.

$$V_C = f_{ce}(bw)\sin\theta_s \tag{8}$$

Truss mechanism resistance V_T

In a coupling beam, the distributed bond stress of beam longitudinal bars and the tensile force of transverse reinforcement generate the inclined compression stress field, which contributes to shear resistance. Thus, the truss mechanism is formed by the inclined compression field of concrete and transverse reinforcement. Thus, the shear strength developed by beam longitudinal bars can be defined as follows:

$$V_{T1} = \left(A_s f_y + \alpha_c A_w f_{yw}\right)\tan\theta_t \tag{9}$$

where α_c = factor related to cut-off bars (= 0.6 for cut-off distributed longitudinal web bars due to insufficient anchorage length, otherwise, 1.0); A_w = area of the distributed longitudinal bars in the web of the beam section; f_{yw} = yield strength of the distributed longitudinal web bars; and θ_t = crack angle in the compression field.

$$\theta_t = \max\left[\theta_s, 26.5°\right] \tag{10}$$

where the crack angle (θ_t) is assumed to be the greater of the diagonal strut angle (θ_s) and 26.5° ($\cot\theta_t$ = 2.0, according to bearing pressure (or compressive stress) distribution in the compression field) (ACI, 2019).

On the other hand, the shear strength of the truss mechanism can be determined by the strength of transverse reinforcement.

$$V_{T2} = A_t f_{yt} n_t = A_t f_{yt} \frac{d}{s \cdot \tan\theta_t} \tag{11}$$

where n_t = the number of transverse reinforcement layers crossing the inclined web crack; d = effective depth of the coupling beam; and s = spacing of the stirrups.
Thus, the shear strength of the truss mechanism is determined by the smaller of V_{T1} and V_{T2}:

$$V_T = \min\left[V_{T1}, V_{T2}\right] \tag{12}$$

Diagonal bar resistance V_D

Existing test results show that large tensile plastic deformation of diagonal bars is developed under cyclic loading. Due to the residual tensile strain, the compressive stress of diagonal bars can be developed early under reversed loading, even under tensile strain. Thus, the shear resistance of the diagonal bars can be contributed by both tension and compression diagonal bars (ACI, 2019).

$$V_D = 2A_d f_{yd}\sin\theta_d \tag{13}$$

MOMENT-ROTATION RELATIONSHIP OF PLASTIC HINGE MODEL

In the proposed model, rotational spring elements (i.e. plastic hinge elements) are used at the interface between beam and wall (**Fig. 2(a)**). The moment-rotation relationship of the rotational spring element is defined as shown in **Fig. 2(b)**: EY (0, M_n), EU (θ_u , M_n), ER (θ_r , 0.2 M_n), and EF (θ_f , 0.2 M_n) indicate the yield, ultimate, residual, and failure points, respectively. The strength (M_n) of EY and EU is defined as the flexural strength of the beam. The deformation (θ_u) of EU is defined by the proposed shear strength degradation model.

Yielding Point

At the yielding point EY, the plastic chord rotation is zero. The nominal flexural strength (M_n) is defined as follows:

$$M_n = \left(A_s f_y + A_d f_{yd}\cos\theta_d\right)\left(d - \frac{c_b}{2}\right) \tag{14}$$

Ultimate Point

In Eqs. (7) and (8), as the shear distortion increases, V_C decreases. On the other hand, V_T and V_D are maintained at uniform values, regardless of the inelastic deformation. Thus, the inelastic shear distortion (γ_u) at the ultimate point can be derived from the degradation of diagonal strut strength (V_C) in Eq. (8): When shear strength degradation occurs, the ultimate point is defined as the intersection point between the shear capacity and the shear demand (i.e. V_f corresponding to M_n). Thus, from V_n (= V_C + V_T + V_D)= V_f and Eqs. (8)-(12), the shear distortion (γ_u) at the ultimate point can be defined as follows:

$$\gamma_u = \frac{1}{85\tan\theta_s}\left[\frac{f_c'(bw)\sin\theta_s}{V_f - V_T - V_D} - 0.8 - 170\varepsilon_{yt}\right] \tag{15}$$

$$V_f = \frac{2M_n}{l} \tag{16}$$

Note that the proposed method considers only shear strength degradation after flexural yielding, and does not consider flexural strength degradation.

At the ultimate point EU, the plastic chord rotation (θ_u) in the plastic hinge is the same as the inelastic shear distortion (γ_u).

$$\theta_u = \gamma_u \tag{17}$$

Residual Point and Failure Point

In the proposed model, a linear strength degradation is assumed between EU and ER. The residual point ER (θ_r , $0.2M_n$) and failure point EF (θ_f , $0.2M_n$) were simplified, on the basis of the strength degradation trend of existing test results.

$$\theta_r = \theta_u + 0.01 \text{ rad.} \tag{18}$$

$$\theta_f = \theta_u + 0.03 \text{ rad.} \tag{19}$$

COMPARISON BETWEEN TEST RESULTS AND PREDICTIONS

Fig. 4 shows the predictions of the proposed model and ASCE/SEI 41-17 (2017) for existing coupling beam specimens using conventional reinforcement. In the predictions of the proposed model, the chord drift ratios (δ_y, δ_u, δ_r, and δ_f) at EY, EU, ER, and EF were calculated as follows:

$$\delta_y = \frac{1 + 20(h/l)^3}{3.6}\frac{V_f l^2}{E_c I_g} \tag{20a}$$

$$\delta_u = \delta_y + \theta_u \tag{20b}$$

$$\delta_r = \delta_u + 0.01 \text{ rad.} \tag{20c}$$

$$\delta_f = \delta_u + 0.03 \text{ rad.} \tag{20d}$$

Fig. 4 compares the prediction results of the proposed model with the test results of specimens with conventional reinforcement layout. The predictions agreed with the test results. On the other hand, ASCE/SEI 41-17 (2017) tended to underestimate the deformation capacity of specimens with conventional reinforcement.

Fig. 5(b) shows the predicted shear capacity-to-tested shear strength ratio (V_n/V_{test}) at the test result of δ_{utest} (at ultimate point) (Eq. (2)). The tested deformation δ_{utest} at the ultimate point was defined as the average of the post-peak lateral drift ratios corresponding to the nominal flexural strength (**Fig. 5(a)**). To evaluate the shear capacity of the proposed method (i.e. V_n = V_C + V_T + V_D (Eqs. (8)-(12)), the inelastic shear distortion ($\gamma = \delta_{utest} - \delta_y$) calculated from δ_{utest} was applied to the proposed method (Eq. (7)). In **Fig. 5(b)**, for the given δ_{utest}, the V_n/V_{test} ratio was close to 1.0, which indicates that the predicted shear capacity V_n agrees with the tested shear strength at the ultimate point EU. **Fig. 5(c)** compares the predicted δ_{upred} with the test result δ_{utest} at the ultimate point EU. The $\delta_{upred}/\delta_{utest}$ ratio shows the average ratio = 1.04 and coefficient of variation (COV) = 0.25. On the other hand, as the δ_{utest} increased, ASCE/SEI 41-17 (2017) underestimated the test result δ_{utest} (average $\delta_{upred}/\delta_{utest}$ ratio = 0.74 and COV = 0.33) (**Fig. 5(d)**).

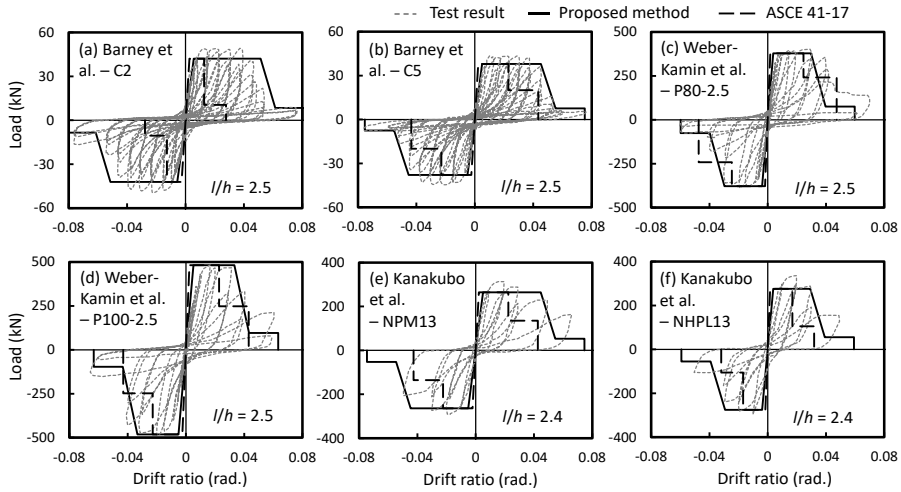

Fig. 4 Comparisons between predictions and test results for coupling beams with conventional longitudinal top and bottom bars

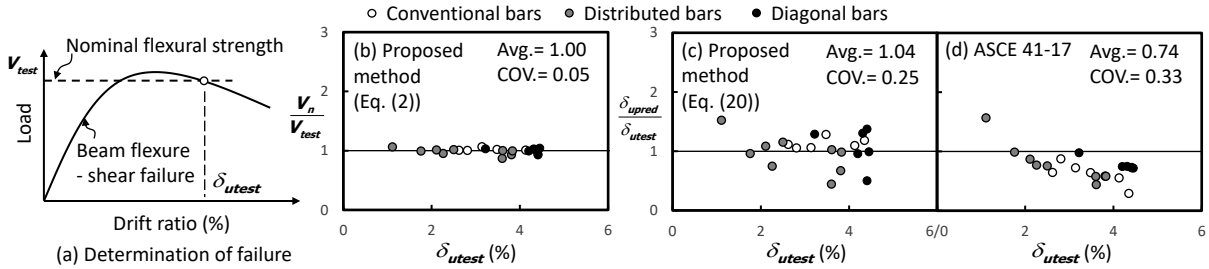

Fig. 5 Comparison between story drift ratio at ultimate point and target drift ratio

CONCLUSIONS

In the present study, a plastic hinge model was developed for the nonlinear numerical analysis of short coupling beams ($l/h \leq 2.5$) with various reinforcement details: conventional, distributed, and/or diagonal bars. The shear strength of the coupling beam was defined as the sum of the contributions by the diagonal strut mechanism, truss mechanism, and diagonal bar resistance. On the basis of the proposed shear strength model, a moment-chord rotation relationship of the rotational spring element was developed to describe the shear strength degradation after flexural yielding. The deformation capacity at the ultimate point was defined at the intersection between the shear capacity curve and shear demand curve. Envelope curves predicted by the proposed method were compared with existing test results. The proposed method agreed with the test results.

ACKNOWLEDGEMENTS

This work is supported by the National Research Foundation of Korea (NRF) grant funded by the Korea government (MSIT) (No. 2020R1F1A1076322, No. 2021R1A4A3030117).

REFERENCES

ACI (American Concrete Institute) (2019), "Building Code Requirements for Structural Concrete and Commentary", ACI 318-19, Farmington Hills, MI.

ASCE 41 (2017), "Seismic Rehabilitation of Existing Buildings (ASCE/SEI 41-17)," American Society of Civil Engineers, Reston, VA, 416 pp.

Eom, T.-S., Park, H.-G., and Kang, S.-M. (2009), "Energy-Based Cyclic Force-Displacement Relationship for Reinforced Concrete Short Coupling Beams," Engineering Structures, V. 31, pp. 2020-2031.

Eom, T.-S. and Park, H.-G. (2013), "Evaluation of Shear Deformation and Energy Dissipation of Reinforced Concrete Members Subjected to Cyclic Loading," ACI Structural Journal, V. 110, No. 5, pp. 845-854.

Eom, T.-S. Lee, S.-J., Kang, S.-M, and Park, H.-G. (2022), "Nonlinear Modeling Parameters of Reinforced Concrete Coupling Beams," ACI Structural Journal, V. 119, No. 2, pp. 89-101.

FEMA 356 (2000), "Prestandard and Commentary for the Seismic Rehabilitation of Buildings," Federal Emergency Management Agency.

Godínez, S.E., Richards, T.L., and Restrepo, J.I. (2021), "Stiffness Modifiers for Diagonally Reinforced Coupling Beams," ACI Structural Journal, V. 118, No. 6, pp. 215-224.

Hong, S.-G., and Jang, S.-K. (2006), "The Mechanism of Load Resistance and Deformability of Reinforced Concrete Coupling Beams (in Korean)", Journal of the Earthquake Engineering Society of Korea, V. 10, No. 3, pp. 113-123.

Hwang, H.-J., Eom, T.-S., and Park, H.-G. (2017), "Shear strength degradation model for performance-based design of interior beam-column joints," ACI Structural Journal, V. 114, No. 5, pp. 1143-1154.

Hwang, H.-J., and Park, H.-G. (2019), "Requirements of shear strength and hoops for performance-based design of interior beam-column joints," ACI Structural Journal, V. 116, No. 2, pp. 245-256.

Hwang, H.-J., and Park, H.-G. (2020), "Performance-based shear design of exterior beam-column joints with standard hooked bars." ACI Structural Journal, V. 117, No. 2, pp. 67-80.

Hwang, H.-J., and Park, H.-G. (2021), "Plastic Hinge Model for Performance-Based Design of Beam-Column Joints," Journal of Structural Engineering, ASCE, V. 147, No. 2, 2021, pp. 04020336.

Kanakubo, T., Fujisawa, M., Sako, N., and Sonobe, Y. (1996), "Ductility of Short Span Beams," Proceedings of the 11th world conference on earthquake engineering, Paper no. 1369.

Lee J.-Y. and Watanabe F. (2003), "Predicting the Longitudinal Axial Strain in the Plastic Hinge Regions of Reinforced Concrete Beams subjected to Reversed Cyclic Loading," Engineering Structures, V. 25, No. 7, pp. 927-939.

Lim, E., Hwang, S.-J., Wang, T.-W., and Chang, Y.-H. (2016), "An Investigation on the Seismic Behavior of Deep Reinforced Concrete Coupling Beams," ACI Structural Journal, V. 113, No. 2, pp. 217-226.

Lim, E., Hwang, S.-J., Cheng, C.-H., and Lin, P.-Y. (2016), "Cyclic Tests of Reinforced Concrete Coupling Beam with Intermediate Span-Depth Ratio," ACI Structural Journal, V. 113, No. 3, pp. 515-524.

Naish, D., Fry, A., Klemencic, R., Wallace J. W. (2013), "Reinforced concrete coupling beams—Part I: Testing," ACI Structural Journal, V. 110, No. 6, pp. 1057–1066.

Naish, D., Fry, A., Klemencic, R., Wallace J. W. (2013), "Reinforced concrete coupling beams—Part II: Modeling," ACI Structural Journal, V. 110, No. 6, pp. 1067–1075.

Vecchio, F.J., and Collins, M.P. (1986), "Modified Compression-Field Theory for Reinforced Concrete Elements Subjected to Shear", ACI Structural Journal, V. 83, No. 2, pp. 219-231.